Iranica Journal of Energy & Environment 3 (1): 23-34, 2012
ISSN 2079-2115
IJEE an Official Peer Reviewed Journal of Babol Noshirvani University of Technology
DOI: 10.5829/idosi.ijee.2012.03.01.0130

BUT

Equilibrium, Thermodynamic and Kinetic Studies on Adsorption of a Basic Dye by Citrullus Lanatus Rind

Bharathi Kandaswamy Suyamboo and Ramesh Srikrishna Perumal

Department of Civil Engineering, National Institute of Technology,
Tiruchirappalli-620 015, Tamil Nadu, India

(Received: December 15, 2011; Accepted: January 21, 2012)

Abstract: An effective biosorbent was developed from Citrullus Lanatus Rind and its various biosorption characteristics were studied for removing a basic dye (Crystal Violet) from its aqueous solution. A series of experiments were conducted in a batch system to assess the effects of the system variables such as contact time, biosorbent dosage, pH, initial dye concentration, temperature, particle size and agitation speed. The biosorbent studied exhibits high efficiency for crystal violet adsorption and the equilibrium states could be achieved in 180 min for the different initial concentrations. The equilibrium adsorption data were analyzed by the Langmuir, Freundlich, Tempkin and Harkins-Jura isotherm models. The equilibrium data indicates the following order to fit the isotherms: Freundlich > Tempkin > Harkins-Jura isotherm > Langmuir. The maximum dye adsorption capacity was found to be 11.99 mg/g at 50°C. The biosorption kinetics was found to follow pseudo-second-order rate kinetic model, with good correlation ($R^2 = 0.99$) and the intra particle diffusion as one of the rate determining steps. Different thermodynamic parameters, like Gibb's free energy (ΔG), enthalpy (ΔH) and entropy (ΔS) of the adsorption process have also been evaluated. The thermodynamic parameters of crystal violet biosorption indicated, the process was spontaneous and endothermic. The results indicated that the biosorbent studied was found to be a promising alternative for the adsorption of crystal violet from aqueous solution.

Key words: Citrullus Lanatus Rind · Crystal Violet · Biosorption · Kinetics · Equilibrium · Thermodynamic

INTRODUCTION

Dyes are organic compounds consisting of two main groups of compounds, chromophores (responsible for color of the dye) and auxochromes (responsible for intensity of the color) [1]. Dyes usually have synthetic origin and complex aromatic molecular structures which make them more stable and more difficult to biodegrade [2]. It is estimated that 10 -15% of the dye is lost in the effluent during the dyeing process [3, 4]. Removal of synthetic dyes from wastewater before discharging to environment and from raw wastewater before offering it to public use is essential for the protection of health and environment [5]. Most of the dyes are toxic and carcinogenic compounds; they are also recalcitrant and thus stable in the receiving environment, posing a serious threat to human/animal health which is not only limited to themselves but may be passed onto further generations by the way of genetic mutations, birth defects, inherited diseases and so on [6]. Many treatment processes such as photocatalytic degradation [7, 8], electrochemical degradation [9], cation exchange membranes [10], micellar enhanced ultra filtration [11], adsorption/ precipitation processes [12], Fenton-biological treatment [13] have been applied for the removal of dyes from wastewater. Adsorption has proven to be more versatile and efficient compared to conventional physico-chemical methods of dye removal [14]. The utilization of waste materials is increasingly becoming of vital concern because these wastes represent unused resources and, in many cases, present serious disposal problems. During the past decade, a great deal of attention has been given to

Corresponding Author: Bharathi Kandaswamy Suyamboo, Department of Civil Engineering, National Institute of Technology, Tiruchirappalli- 620 015, Tamil Nadu, India.
Tel: +91-431-250-3166.

methods of converting these materials into useful products [15]. Consequently many investigators have studied the feasibility of using low cost sorbents such as: coconut husk [16, 17], wheat bran [18], vetiver roots [19], cotton stalk and its hull [20], date stones [21, 22], pistachio nut shell [23], apple promace and wheat straw [24]. The aim of the present study is to explore the capability of Citrullus Lanatus Rind to remove basic dye, crystal violet, from aqueous solution under different experimental conditions such as contact time, biosorbent dosage, pH, initial dye concentration, temperature, particle size and agitation speed. The adsorption kinetic models, equilibrium isotherm models and thermodynamic parameters were also evaluated.

MATERIALS AND METHODS

Preparation and Characterization of Biosorbent: Citrullus Lanatus Rinds (CLR) was collected from the market as solid waste in Tiruchirappalli, Tamil Nadu, India. The rinds were thoroughly washed with distilled water to remove the dirt adhered at the surface. Then it was sliced, spread on trays and kept under hot sun for 5 days. The dried biomass was ground, sieved and stored in air tight container for further use. No other physical or chemical treatments were given prior to adsorption experiments.

Table 1 shows the biosorbent characteristics like specific gravity, density, iodine number, loss on ignition and point of zero charge (pH_{zpc}). The pH_{zpc} was determined using the solid addition method [25]. Scanning Electron Microscopy (SEM) analysis was carried out on the CLR to study the surface morphology before and after adsorption. The surface functional groups of the loaded and unloaded biosorbent were detected by Fourier Transform Infrared (FTIR) spectroscope. The spectra were recorded from 4000 - 400 cm^{-1}.

Preparation of Adsorbate Solutions: Crystal Violet (CV) used in this study was procured from S. D. Fine-Chem. Ltd. (India) (CI 42555, MF: $C_{25}H_{30}ClN_3$, λmax: 579 nm) and used without further purification. The molecular structure of the dye is illustrated in Fig.1. Dye stock solution (1000 mgL^{-1}) was prepared by dissolving accurately the weighed quantity of the dye in doubled distilled water. Experimental dye solution of different concentrations was prepared by diluting the stock solution with suitable volume of double distilled water.

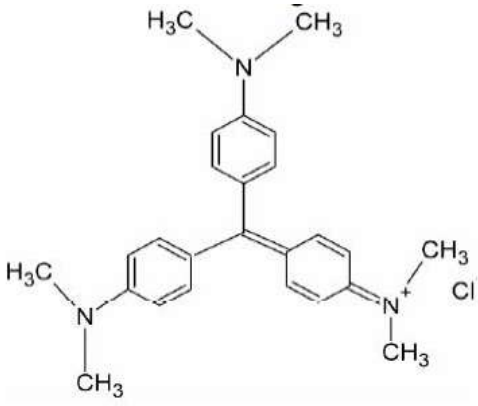

Fig. 1: Molecular structure of Crystal Violet (CV)

Instruments Used for Characterization: Unknown concentration of dye was determined by finding out the absorbance at the characteristic wavelength using a double beam UV/visible spectrophotometer (Lambda 25). The pH measurements were carried out using an Orion EA 940 expandable ion analyzer. An IHC- 3280 Orbital shaking incubator was used for all adsorption experiments. Centrifuge was done by TC 650 S multispin centrifuge. Fourier Transform Infrared Spectrometer (FTIR- 2000, Perkin-Elmer) was used to analyze the organic functional group of the biosorbent. A Scanning Electron Microscope (HITACHI S-3000H) was used to examine the surface morphology of the biosorbent.

Biosorption Studies: Biosorption of crystal violet by CLR was carried out by batch method and the influence of various parameters such as contact time (5-210 min), biosorbent dosage (0.1-1.2 g/L), pH (2-12), initial dye concentration (10 - 30mg/L), temperature (30°C - 50°C), particle size (<150µm, 150 - 300µm, 300 - 600µm) and agitation speed (50-200 rpm) were studied. The adsorption measurements were conducted by mixing various amounts of CLR in glass Erlenmeyer flasks containing 50 mL of dye solution of known concentration. The pH of the solution was adjusted to the desired value by adding small amount

Table 1: Characteristics of the biosorbent

Biosorbent	Specific Gravity	Density(g/cc)	Moisture content (%)	Iodine number	Loss on Ignition (%)	pH_{zpc}
Citrullus Lanatus Rind	0.67	0.222	6.98	510	84.42	6.4

of HCl or NaOH (0.1M). The solutions were agitated using orbital shaker for a predescribed time to attain equilibrium. At the end of predetermined time intervals, the samples were taken out and the supernatant solution was separated from the CLR by centrifugation at 10000 rpm for 5 min and the percentage removal of dye was calculated as:

$$\text{Romoval } \% = \frac{C_0 - C_t}{C_0} \quad (1)$$

where C_o is the initial concentration of the dye (mg/L) and C_t is the concentration of the dye (mg/L) at time t.

The effect of temperature on the adsorption characteristics was studied to determine the thermodynamic parameters. Adsorption isotherms were investigated by the Langmuir, Freundlich, Tempkin and Harkins-Jura models and the reaction kinetics was performed by first order and second order kinetics.

RESULTS AND DISCUSSION

Characterization of Biosorbent: The characteristics of the biosorbent like specific gravity, density, iodine number, loss on ignition and pH_{zpc} were examined and listed in Table 1.

The result of the point of zero charge of the biosorbent is presented in Fig. 2. From the Fig. 2, it was observed that at pH below 6.4 the surface of the CLR is predominated by positive charges while at pH greater than 6.4 the surface is predominated by negative charges.

The surface morphology of the CLR before and after dye biosorption has been studied by Scanning Electron Microscope technique and the results are shown in Fig. 3. It is clear that CLR has considerable number of heterogeneous layer of pores where there is a good possibility of dye to be adsorbed.

The FT-IR spectra of CLR before and after biosorption were performed in the range of 400- 4000cm^{-1} in order to explore the surface characteristics of the biosorbent (Fig. 4(a) and 4(b)). The spectra display a number of adsorption peaks, indicating the complex nature of CLR. The peak positions were noticed at 3929.84, 3820.95, 3706.86, 3389.93, 3285.60, 2929.25, 2239.66, 1634.19, 1430.29, 1247.20 and 1057.0 cm^{-1}. The band at 3929.84 cm^{-1} is due to O-H stretch vibration that is present on the biosorbent [26]. The band observed at about 2929.25 cm^{-1} could be assigned to CH stretch shift [27]. The peak present at 1430.29 cm^{-1} represents the CH_2 deformation [27]. The peak around 1634.19 corresponds to C=O stretch [28]. While the band at 1247.20 cm^{-1} corresponds to Si-C stretch [29] and the band at 1057.0 cm^{-1} represents C-OH stretching vibrations deformation [30]. Comparing Fig. 4(a) and 4(b), we can conclude that some of these peaks are shifted or disappeared and new peaks are also detected. These changes observed in the spectrum, indicated the possible involvement of those functional groups on the surface of the CLR in sorption process.

Effect of Contact Time and Initial Dye Concentration: The effluent of different industries may have different dye concentrations. Initial dye concentration is one of the important factors that affect adsorption kinetics. The effect of initial dye concentration onto CV biosorption by CLR was studied at different initial concentrations (10, 20 and 30 mg/L) at 30°C and the results are shown in Fig. 5. It can be seen that the percentage of dye adsorbed increased with increase in concentration. As the initial concentration increased from 10 - 30 mg/L, the percentage removal increased from 87% to 91%. This is due to the fact that increase in concentration enhances the interaction between the dye and adsorbent apart from providing necessary driving force to overcome the resistance to mass transfer of dye [31]. Fig. 5 also indicated that the dye uptake increased with time and, at some point in time, reached a constant value where no more dye was removed from the solution. The equilibrium time was found to be 180 min for all the initial concentrations studied. However the rapid adsorption observed during the first 5 min is probably due to the abundant availability of active sites on the surface of the adsorbent.

Biosorption Kinetics: Several kinetic models have been used to investigate the mechanism of process and the potential rate-controlling steps involved in the process of biosorption. In this study, the mechanism of biosorption was investigated by the kinetic models such as pseudo-first-order [32], pseudo-second-order [33] and intraparticle diffusion model [34]. The linear forms of the above models are given in Eqns. (2), (3) and (4) respectively:

$$\log\left(q_e - q_t\right) = \log\left(q_e\right) - \frac{k_1}{2.303} \quad (2)$$

$$\left(\frac{t}{q_t}\right) = \frac{1}{k_2 q_e^2} + \frac{1}{q_e}(t) \quad (3)$$

$$q_t = k_{id}\, t^{\frac{1}{2}} + C \quad (4)$$

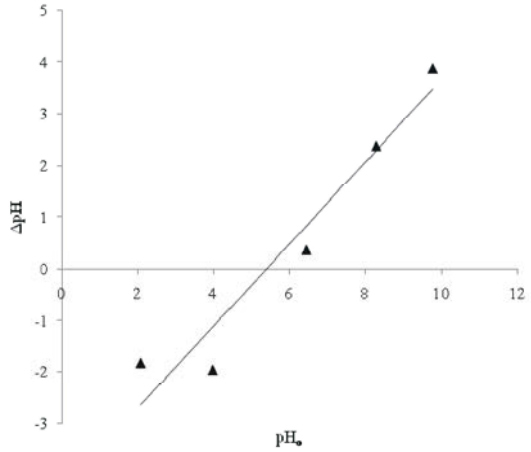

Fig. 2: Point of Zero Charge for Citrullus Lanatus Rind

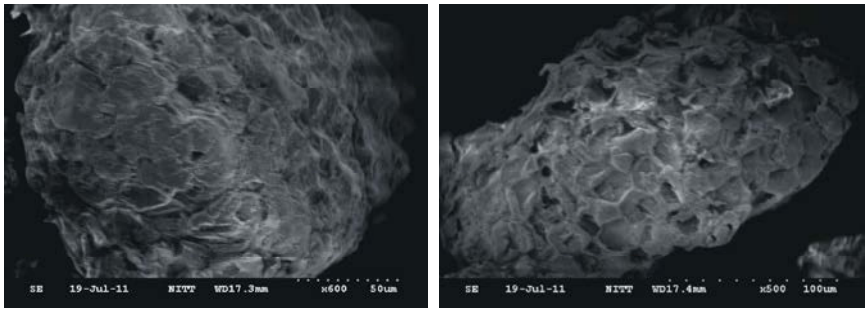

(a) (b)

Fig. 3: SEM micrographs: (a) raw biosorbent and (b) CV dye loaded biosorbent

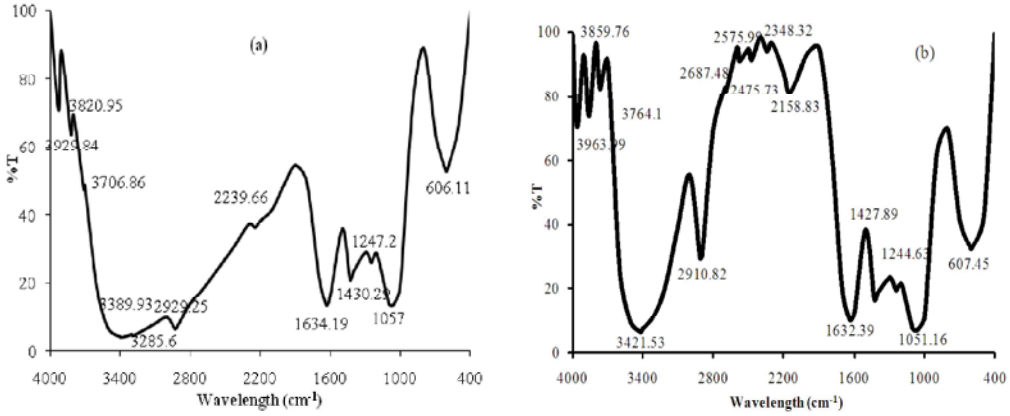

Fig. 4: FT-IR spectrum of CLR: (a) raw biosorbent (b) CV dye loaded biosorbent.

Where q_t and q_e (mg/g) are the adsorption capacities at time t and at equilibrium respectively; k_1 (l/min) and k_2 (mg/ (g min)) are the pseudo-first and pseudo-second order rate constants; k_{id} is the intraparticle diffusion rate constant (mg/ ($gmin^{0.5}$)) and C is the intercept which gives an idea about the boundary layer thickness.

The effect of contact time and initial dye concentration was investigated to find the best kinetic model. In all the conditions studied, the pseudo- first-order equation did not fit well to the whole range of concentrations. It can be seen (Table 2) that for the first order kinetics though the correlation coefficient values are high (> 0.80), the experimental q_e values do not agree with the q_{cal} calculated

Table 1: Characteristics of the biosorbent

Biosorbent	Specific Gravity	Density(g/cc)	Moisture content (%)	Iodine number	Loss on Ignition (%)	pH_{zpc}
Citrullus Lanatus Rind	0.67	0.222	6.98	510	84.42	6.4

Table 2: Kinetic parameters for biosorption of CV onto CLR

Temperature	Langmuir isotherm constants			Freundlich isotherm constants			Tempkin isotherm constants			Harkins-Jura isotherm constants		
(°C)	q_{max} (mg/g)	b(L/mg)	R^2	K (mg/g)	n	R^2	AT(L/mg)	BT	R^2	A	B	R^2
30	-21.74	-0.186	0.85	4.82	0.70	0.90	1.525	8.366	0.95	14.70	0.35	0.85
40	-166.67	-0.058	0.98	10.49	0.92	0.98	2.725	11.71	0.94	10.10	0.13	0.83
50	38.46	0.464	0.97	11.99	1.24	0.98	3.00	12.76	0.87	25.64	0.30	0.86

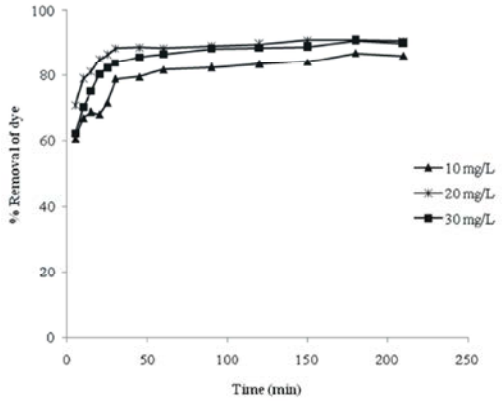

Fig. 5: Effect of contact time on biosorption of CV by CLR at different initial dye concentration (biosorbent dosage= 1g/L; particle size=150-300µm; agitation speed=150 rpm; temperature=30°C)

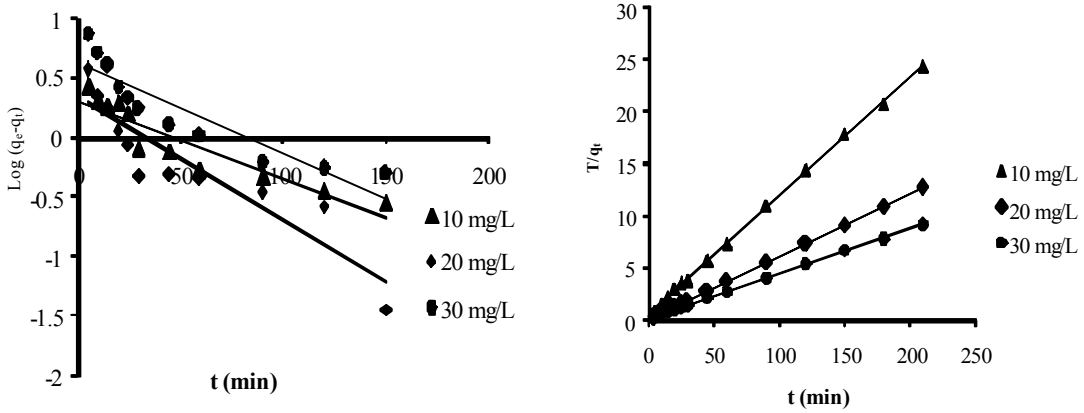

Fig. 6: (a) Pseudo-first-order (b) Pseudo-second-order kinetic plots for biosorption of CV onto CLR at different initial concentrations (particle size=150-300µm; agitation speed=150 rpm; temperature =30°C)

from the linear plots. This shows that the biosorption of CV onto CLR did not follow first-order kinetic, indicating that the sorption was not diffusion-controlled and adsorption was not preceded by diffusion through a boundary [35]. This is confirmed by results obtained with the intraparticle model. In this model, the plot was not linear over the whole time range, which indicated that more than one process affected adsorption. The intra particle diffusion plot shows that the adsorption occurs in two steps. The first linear portion indicates that boundary layer diffusion probably limited CV adsorption [36]. The second linear portion is a delay process that corresponds to intra-particle diffusion.

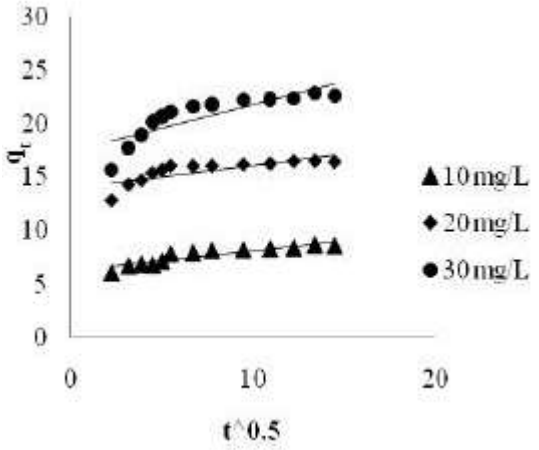

Fig. 7: Intraparticle diffusion plot for different initial dye concentrations on biosorption of CV by CLR (biosorbent dosage = 1g/L; agitation speed = 150 rpm; temperature = 30°C)

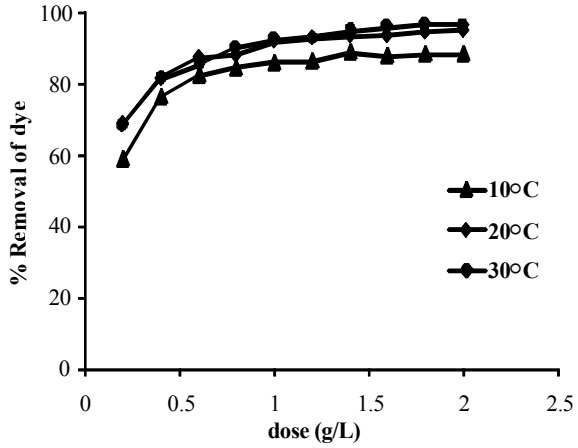

Fig. 8: Effect of biosorbent dosage on biosorption of CV by CLR at different temperature (equilibrium time = 180 min; C_o = 10 mg/L; particle size=150-300µm; agitation speed=150 rpm)

But the intra- particle diffusion rate increased with initial CV concentration. Similar kinetic behavior has also been reported for the biosorption of basic dye onto other low cost adsorbents such as papaya seeds [37], pistachio hull [38]. The correlation coefficients for the pseudo-second-order-kinetics are closer to unity than that of the pseudo-first-order kinetics. Also the $q_{e,exp}$ and the $q_{e,cal}$ values of the pseudo-second-order kinetic model are closer to each other. This suggests that the sorption system can be well represented by the pseudo-second-order model for the adsorption of CV by CLR. The linear plots of the models are represented in Fig. 6 (a), 6(b) and Fig. 7 respectively.

Effect of Biosorbent Dosage and Temperature: The effect of biosorbent dosage on CV removal was studied by increasing the dose of CLR keeping the initial CV concentration (10 mg/L) as constant at equilibrium time for different temperature. From Fig. 8 it is clear that the percentage adsorption increased with the increase in adsorbent dosage. This can be due to the fact that, the active sites could be effectively utilized when the dosage was low [31]. But the amount of dye adsorbed per unit weight of the adsorbent decreases with increase in dosage. This may be attributed to the aggregation of adsorbent particles at high dosage, which reduces the total surface area of the adsorbent and results in an increase in the diffusion path length [39].

The uptake of CV increased as the temperature is raised from 30 to 50^{0}C. The maximum removal was found to be 89, 95 and 97% at a dose of 1.4g/L, 1.8g/L and 1.8g/L for a temperature of 30, 40 and 50^{0}C respectively. This is due to the fact that, at higher concentration of the adsorbent, there is a very fast superficial adsorption onto the adsorbent surface that produces a lower solute concentration in the solution than when CLR dose is lower. Thus, with increasing adsorbent dose, the amount of CV adsorbed per unit mass of CLR is reduced, thus causing a decrease in q_e value [40].

Biosorption Isotherms: Isotherms correlate the equilibrium adsorption data with different mathematical models to describe how adsorbate interacts with adsorbents and is critical in optimizing the use of adsorbents. The fitness of the equilibrium data obtained from the experiments at different temperatures was evaluated with the Langmuir, Freundlich, Tempkin and Harkins-Jura isotherm models.

The Langmuir isotherm assumes that adsorption takes place at specific homogeneous sites within the adsorbent and there is no significant interaction among the adsorbed species. Also, the adsorption rate is proportional to the number of free sites on the adsorbent and fluid concentration. Once a dye molecule occupies a site, no further adsorption will take place at the site [41]. The linear Langmuir equation can be represented as

$$\frac{1}{X/M} = \frac{1}{q_{\max}} + \frac{1}{q_{\max} b}\frac{1}{C_e} \qquad (5)$$

Where q_{max} is the maximum monolayer dye concentration in the solid phase (mg/g), C_e is the equilibrium dye concentration in the aqueous phase (mg/L), X/M = q_e is the equilibrium dye concentration in

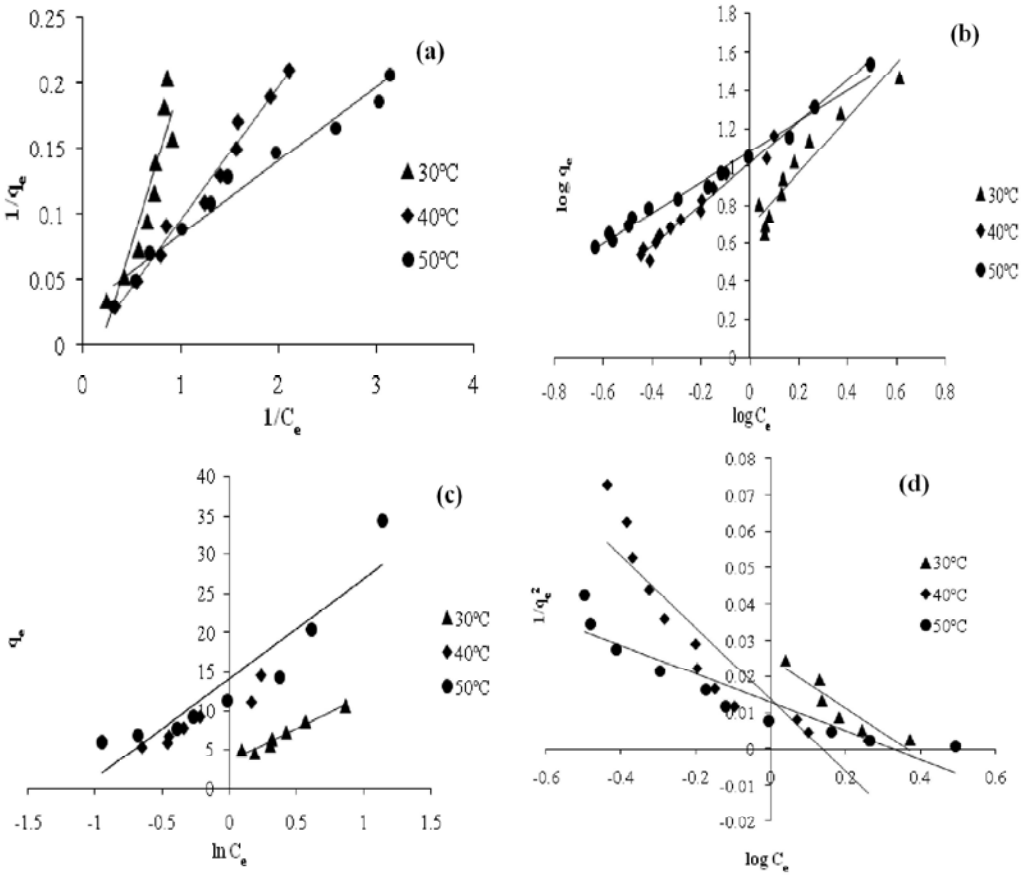

Fig. 9: (a) Langmuir isotherm (b) Freundlich isotherm (c) Tempkin isotherm (d) Harkins- Jura isotherm plots for different temperatures on the biosorption of CV by CLR (C_o= 10 mg/L; particle size=150-300µm; agitation speed=150 rpm)

Table 3: Adsorption kinetic model rate constants for CV removal

		Pseudo-first-order-kinetic model			Pseudo-second-order kinetic model			Intra-particle diffusion model		
C_0	q_e (exp) (mg/g)	qe (cal)(mg/g)	k_1 (min^{-1})	R^2	q_e (cal) (mg/g)	K_2(min^{-1})	R^2	K^{id}(mg/gmin$^{0.5}$) (mg/g)	C	R^2
10	8.70	1.99	0.014	0.86	8.77	0.026	0.99	0.189	6.237	0.83
20	16.51	2.123	0.023	0.84	16.66	0.036	0.99	0.160	14.41	0.72
30	23.0	4.12	0.016	0.83	23.25	0.015	0.99	0.457	17.4	0.76

the solid phase (mg/g) and b is the Langmuir equilibrium constant (L/mg). Fig. 9a shows the Langmuir ($1/q_e$ vs $1/C_e$) plots for adsorption of CV at different temperatures. The values of q_{max}, b and the correlation coefficients for Langmuir isotherm are presented in Table 3.

The Freundlich equilibrium isotherm [42] was also used to describe the experimental adsorption data. This isotherm model assumes a heterogeneous surface with a non-uniform distribution of heat of adsorption over the surface. The Freundlich isotherm can be expressed by [43].

$$\log q_e = \log k + \frac{1}{n} * \log C_e \quad (6)$$

where K and n are Freundlich constants related to adsorption capacity and adsorption intensity respectively. These constants can be obtained from the plot of log q_e versus log C_e. From Fig. 9b a linear relationship was observed among the plotted parameters at different temperatures. The isotherm constants along with correlation coefficients (R^2) are presented in Table 3. Comparing the R^2 values of both the isotherms, the equilibrium data fitted well with the Freundlich isotherm for dye sorption at the different studied temperatures.

The Tempkin equation suggests a linear decrease of sorption energy as the degree of completion of the sorptional centers of an adsorbent is increased.

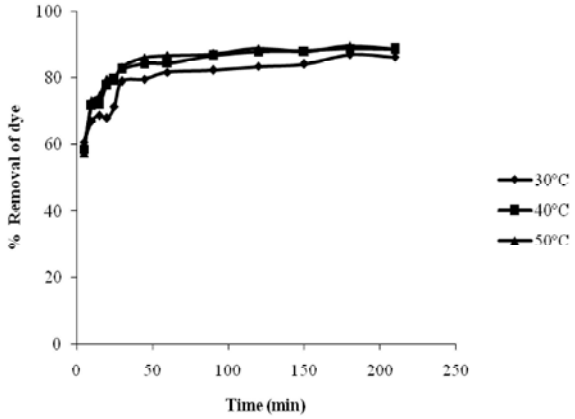

Fig. 10: Effect of temperature on CV biosorption by CLR (C_o= 10 mg/L; biosorbent dosage = 1g/L; particle size=150-300µm; agitation speed=150 rpm)

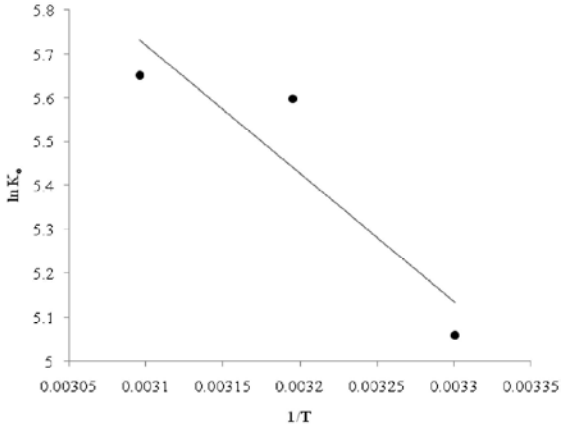

Fig. 11: Von't Hoff plot for effect of temperature on biosorption of CV onto CLR.

The heat of adsorption and the adsorbent-adsorbate interaction on adsorption isotherms were studied by Tempkin and Pyzhev [44]. The Tempkin isotherm equation is given as

$$q_e = B_T (\ln A_T + \ln C_e) \quad (7)$$

where B_T= RT/b, T is the absolute temperature in K, R the universal gas constant, 8.314 J $mol^{-1}K^{-1}$, A_T the equilibrium binding constant (Lmg^{-1}) and B_T is related to the heat of adsorption. A plot of q_e vs ln C_e at studied temperature is shown in Fig. 9c. The Tempkin isotherm constants are given in Table 3. The Tempkin constant, B_T, shows that the heat of adsorption increases with increase in temperature, indicating endothermic adsorption.

The Harkins-Jura adsorption isotherm can be expressed as [45].

$$\frac{1}{q_e^2} = \left(\frac{B}{A}\right) - \left(\frac{1}{A}\right) \log C_e \quad (8)$$

Where B and A are the isotherm constants. The Harkins-Jura adsorption isotherm accounts to multilayer adsorption and can be explained with the existence of heterogeneous pore distribution. The value of $1/q_e^2$ was plotted against log C_e (Fig. 9d). The isotherm constants and correlation coefficients are summarized in Table 3.

Thermodynamic Studies: The effect of temperature on the biosorption of CV onto CLR was investigated under isothermal conditions in the temperature range of 30-50^{0}C. The temperature dependence of CV adsorption on CLR is shown in Fig. 10. The extent of adsorption of CV is found to increase with increase in temperature and time, indicating the process to be endothermic in nature [46]. The increased removal of CV may be attributed to the increase of mobility of the CV particles and the swelling of pore structure of the sorbent [47].

Thermodynamic parameters reflect the feasibility and spontaneous nature of the adsorption process. The thermodynamic parameters such as change in free energy (ΔG) (J $mole^{-1}$), enthalpy (ΔH) (J $mole^{-1}$) and entropy (ΔS) (J K^{-1} $mole^{-1}$) were determined using the following equations:

$$K_o = \frac{C_{solid}}{C_{liquid}} \quad (9)$$

$$\Delta G = \Delta H - T\Delta S \quad (10)$$

$$In\ k_o = \frac{-\Delta G}{RT} \quad (11)$$

$$In\ k_o = \frac{\Delta S}{R} - \frac{\Delta H}{RT} \quad (12)$$

Where K_o is equilibrium constant, C_{solid} is solid phase concentration at equilibrium (mg/l), C_{liquid} is liquid phase concentration at equilibrium (mg/L), T is absolute temperature in Kelvin and R is gas constant.

ΔH and ΔS values are obtained from the slope and intercept of plot ln K_o against 1/T. Fig. 11 illustrates Von't Hoff plot of effect of temperature on biosorption of CV on CLR. The observed thermodynamic values are listed in Table 4. The negative value of ΔG indicates the biosorption is favorable and spontaneous. The high positive values of ΔH confirm the endothermic nature of adsorption process. The positive values of ΔS indicate the increased disorder and randomness at the solid solution interface of CV with the adsorbent.

Table 4: Thermodynamic parameters of CV over CLR

	ΔG (J/mole)				
Initial CV concentration (mg/L)	303K	313K	323K	ΔH(J/mole)	ΔS(J/K/mole)
10	-12458.82	-14245.43	-14841.74	2932	14.81

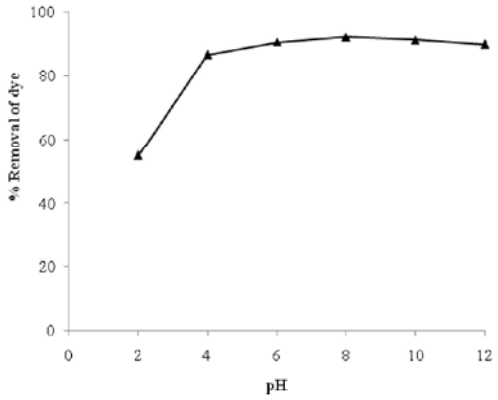

Fig. 12: Effect of pH on biosorption of CV onto CLR (C_0 = 10 mg/L; temperature = 30°C; agitation speed = 150 rpm)

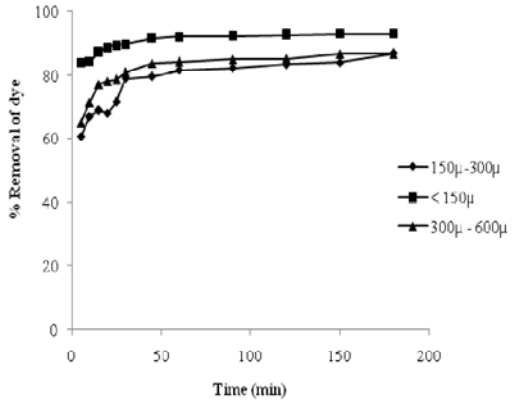

Fig. 13: Effect of particle size on biosorption of CV onto CLR (C_0 = 10mg/L; contact time = 180 min; temperature = 30°C; biosorbent dosage = 1 g/L)

The increase of adsorption capacity of the biosorbent at higher temperatures was due to enlargement of pore size and activation of adsorbent surface [48].

Effect of pH: The pH of the dye solution plays an important role on the adsorption capacity, where it affects both the degree of ionization of the dye as well as the surface binding sites of the adsorbent. The variation of the dye uptake with initial pH was shown in Fig. 12. From the Fig. 12, it was clear that the degree of CV adsorption onto CLR increased from 54.8% to a maximum of 92.0% when the solution pH was increased from 2 to 8. Hence the optimum pH of CV adsorption was taken as 8.0. The reason that CLR behaved differently in adsorbing CV at different solution pH can be explained by considering the pH_{zpc} of the adsorbent as well as molecular nature of CV. The pH_{zpc} of CLR surface is 6.4, meaning that the surface of the adsorbent was positively charged at a solution pH below 6.4. This causes competition between protons and the CV formed cations for adsorption locations [49, 50] as well as the repulsion of cationic CV molecules, resulting in the reduction of dye adsorption. The lower the pH goes below pH_{zpc} the greater the density of positive ions on the surface of CLR will be which in turn for less adsorption. When solution pH increases above pH_{zpc}, a negative charge is present on the surface of CLR causing better CV adsorption through the electro static attraction phenomenon [38].

Effect of Particle Size: Biosorption rate of CV dye for three different particle sizes of CLR (<150, 150-300 and 300-600µm) was studied keeping the other parameters as constant. The results of variation of these particle sizes on dye adsorption rate are shown in Fig. 13. The adsorption efficiency of CLR decreased from 93.06% to 86.84% as the particle size increased from <150 to 300 - 600µm. It can be attributed to the fact that the smaller biosorbent particles have shortened diffusion path and increased total surface area and therefore the ability to penetrate all internal pore structure of the biosorbent is very high [51]. It can be seen from Fig. 13, that the equilibrium time is almost constant for all the selected sizes of the sorbent. From this, it can be concluded that the equilibrium time is dependent on surface characteristics of adsorbent and adsorbate and independent on adsorbent size.

Effect of Agitation Speed: Agitation speed is an important parameter in sorption phenomena, which has a serious action on the distribution of the solute in the bulk solution and the formation of the external boundary film. The effect of agitation on the uptake of CV by CLR was studied at different agitation speeds (50-200 rpm). From Fig. 14, it can be observed that agitation speed significantly affects the biosorption of CV, thus confirming that the influence of external diffusion on the sorption kinetic control plays a significant role.

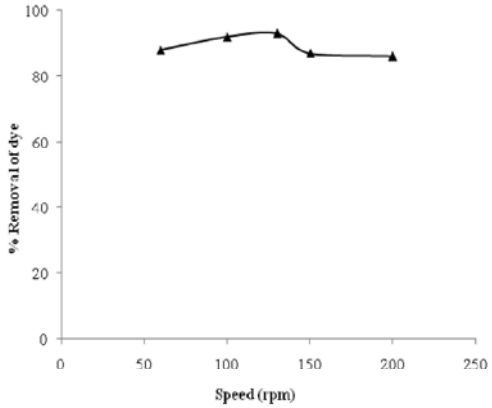

Fig. 14: Effect of agitation speed on biosorption of CV onto CLR (C_0 = 10mg/L; contact time = 180 min; temperature = 30°C; biosorbent dosage = 1 g/L)

The percent of dye adsorbed was found to increase from 88 to 93% with increased in agitation speed from 50 rpm to 130 rpm, thus confirming that the influence of external diffusion on the sorption kinetic control plays a significant role. With increasing the agitation speed, the rate of diffusion of dye molecules from bulk liquid to the liquid boundary layer surrounding the particle becomes higher because of an enhancement of turbulence and a decrease of thickness of the liquid boundary layer [52]. Also it is clear that while increasing the speed from 130 to 200 rpm, the percent removal of dye was decreased to 86%. This decrease in percent removal may be attributed to an increase desorption tendency of dye molecules and/or having similar speed of adsorbent particles and adsorbate ions. This desorption tendency may be attributed to high mixing speed which means more energy input and higher shear force causing break of bonds between CV and the adsorbent [53]. This also indicates that a 130 rpm agitation speed is sufficient to assure that all the surface binding sites are made readily available for dye uptake.

CONCLUSION

The biosorption of CV onto CLR was proven to be an efficient process. The amount of dye adsorbed was found to vary with contact time, biosorbent dosage, pH, initial concentration, particle size, temperature and agitation speed. The maximum uptake of dye by CLR occurred at a pH of 8. The equilibrium adsorption was attained after 180 min. The Langmuir, Freundlich, Tempkin and Harkins-Jura isotherm models were used for the mathematical description of the biosorption equilibrium of CV onto CLR. The Freundlich isotherm model was found to provide the best fit of the experimental data in the temperature range studied. The pseudo-second-order kinetic model agrees well with the dynamical behavior for the adsorption of CV onto CLR under several different initial concentrations. The thermodynamic parameters ΔG (J/mole), ΔH (J/mole) and ΔS (J/K/mole) indicated the endothermic nature of biosorption and the increased randomness at the solid-solution interface during adsorption respectively. Results obtained from this study indicated that CLR could be used as a potential sorbent for the removal of CV from the aqueous solution in a batch system. Since the Citrullus Lanatus Rinds are freely, abundantly and locally available, it can be used as an economical sorbent for the real industrial effluent.

REFERENCES

1. Christie, R., 2001. Color Chemistry, The Royal Society of Chemistry, Cambridge, United Kingdom.
2. Sayan, E., 2006. Optimization and modeling of decolorization and COD reduction of reactive dye solutions by ultrasound-assisted adsorption. Chem. Eng. J., 119: 175-181.
3. Garg, V.K., R. Gupta, A.B. Yadav and R. Kumar, 2003. Dye removal from aqueous solution by adsorption on treated sawdust. Bioresource Technol., 89: 121-124.
4. Young, L. and J. Yu, 1997. Lignase-catalysed decolourisation. Water Res., 31: 1187-1193.
5. Numan, H., B. Edip and A. Erol, 2006. Kinetic and equilibrium studies on the removal of acid dyes from aqueous solutions by adsorption onto activated carbon cloth. J. Hazard. Mater., 137: 344-351.
6. Crini, G., 2008. Kinetic and equilibrium studies on the removal of cationic dyes from aqueous solution by adsorption onto a cyclodextrin polymer. Dyes Pigments. 77: 415-426.
7. Sohrabi, M.R. and M. Ghavami, 2008. A novel agricultural waste adsorbent for the removal of cationic dye from aqueous solutions. J. Hazard. Mater. B., 153: 1235-1239.
8. Sleiman, M., D.L. Vildozo, C. Ferronato and J.M. Chovelon, 2007. Photocatalytic degradation of patent blue v by supported TiO_2: Kinetics, mineralization and reaction pathway. Appl. Catal. B., 77: 1-11.
9. Fan, L., Y. Zhou, W. Yang, G. Chen and F. Yang, 2008. Electrochemical degradation of aqueous solution of Amaranth azo dye on ACF under potentiostatic model. Dyes Pigments. 76: 440-446.

10. Wu, J.S., C.H. Liu, K.H. Chu and S.Y. Suen, 2008. Removal of cationic dye methyl violet 2B from water by cation exchange membranes. J. Membr. Sci., 309: 239-245.
11. Zaghbani, N., A. Hafiane and M. Dhahbi, 2008. Removal of Safranin T from wastewater using micellar enhanced ultrafiltration. Desalination. 222: 348-356.
12. Zaghbani, M.X., L. Lee, H.H. Wang and Z. Wang, 2007. Adsorption of methylene blue on low-cost adsorbents: A review. J. Hazard. Mater., 149: 735-741.
13. Lodha, B. and S. Chaudhari, 2007. Effect of Electro-Fenton application on azo dyes biodegradability. J. Hazard. Mater., 148: 459-466.
14. Senthilkumar, S., P. Kalaamani, K. Porkodi, P.R. Varadarajan and C.V. Subburaam, 2006. Adsorption of dissolved Reactive red dye from aqueous phase onto activated carbon prepared from agricultural waste. Bioresour. Technol., 97: 1618-1625.
15. Jain, A.K., V.K. Gupta, A. Bhatnagar and I.A. Suhas, 2003. Utilization of industrial waste products as adsorbents for the removal of dyes. J. Hazard. Mater., 101(1): 31-42.
16. Tan, I.A.W., A.L. Ahmad and B.H. Hameed, 2008. Agricultural based activated carbons for the removal of dyes from aqueous solutions: A review. J. Hazard. Mater., 154: 337-346.
17. Tamai, H., T. Kakii, Y. Hirota, T. Kumamoto and H. Yasuda, 1996. Synthesis of extremely large mesoporous activated carbon and its unique adsorption for giant molecules. Chem. Mater., 8: 454-462.
18. Ozer, A. and G. Dursun, 2007. Removal of Methylene blue from aqueous solution by dehydrated wheat bran carbon. J. Hazard. Mater., 146: 262-269.
19. Altenor, S., B. Carene, E. Emmanuel, J. Lambert, J.J. Ehrhardt and S. Gaspard, 2009. Adsorption studies of Methylene blue and phenol onto vetiver roots activated carbon prepared by chemical activation. J. Hazard. Mater., 165: 1029-1039.
20. Tunc, O., H. Tanaci and Z. Aksu, 2009. Potential use of cotton plant wastes for the removal of Remazol Black B reactive dye. J. Hazard. Mater., 163: 187-198.
21. Girgis, B., S. Abdel-Nasser and A. El-Hendawy, 2002. Porosity development in activated carbons obtained from date pits under chemical activation with phosphoric acid. Micropor. Mesopor. Mater., 52: 105-117.
22. Haimour, N.M. and S. Emeish, 2006. Utilization of date stones for production of activated carbon using phosphoric acid.Waste Manage., 26: 51-60.
23. Yang, T. and L.A. Chong, 2006. Equilibrium, thermodynamic and kinetic studies on adsorption of commercial dye by activated carbon derived from olive-waste cakes. Mater. Chem. Phys., 100: 438-444.
24. Chandran, B.P., 2002. Nigam, Adsorptive removal of textile reactive dye using Posidonia oceanica (L.) fibrous biomass. Water Res., 36: 2824-2830.
25. Oladoja, N.A. and Y.D. Aliu, 2009. Snail shell as coagulant aid in the alum precipitation of malachite green from aqua system. J. Hazard. Mater., 164: 1496-1502.
26. Elkady, M.F., M.I. Amal and M.M. Abd El-Latif, 2011. Assessment of the adsorption kinetics, equilibrium and thermodynamic for the potential removal of reactive red dye using eggshell biocomposite beads. doi:10.1016/j.desal. 2011.05.063.
27. Hameed, B.H. and M.I. El-Khaiary, 2008. Removal of basic dye from aqueous medium using a novel agricultural waste material: Pumpkin seed hull. J. Hazard. Mater., 155: 601-609.
28. Hameed, B.H. and A.A. Ahmad, 2009. Equilibrium and kinetics study of reactive red 123 dye removal from aqueous solution by adsorption on eggshell. J. Hazard. Mater., 164: 870-875.
29. Hameed, B.H., D.K. Mahmoud and A.L. Ahmad, 2008. Equilibrium modeling and kinetic studies on the adsorption of basic dye by a low-cost adsorbent: Coconut (Cocos nucifera) bunch waste. J. Hazard. Mater., 158: 65-72.
30. Tan, I.A.W., A.L. Ahmad and B.H. Hameed, 2008. Adsorption of basic dye using activated carbon prepared from oil palm shell: batch and fixed bed studies. Desal., 225: 13-28.
31. Ponnusami, V., V. Gunasekar and S.N. Srivastava, 2009. Kinetics of methylene blue removal from aqueous solution using gulmohar (Delonix regia) plant leaf powder: multivariate regression analysis. J. Hazard. Mater., 169: 119-127.
32. Lagergren, S., 1898. Citation review of Lagergren kinetic rate equation on adsorption reactions. Handlingar. 24: 1-39.
33. Ho, Y.S., 1995. PhD thesis, University of Birmingham.
34. Weber, W.J. and J.C. Morris, 1963. Adsorption Characteristics of a Low-Cost Activated Carbon for the Reclamation of Colored Effluents Containing Malachite Green. J. Sanit. Eng. Div. Am. Soc. Civ. Eng., 89: 31-60.
35. Sener, S., 2008. Use of solid wastes of the soda ash plant as an adsorbent for the removal of anionic dyes: Equilibrium and kinetic studies. Chem. Eng. J., 138: 207-214.

36. Dizge, N., C. Aydiner, E. Demirbas, M. Kobya and S. Kara, 2008. Adsorption of reactive dyes from aqueous solutions by fly ash: kinetic and equilibrium studies. J. Hazard. Mater., 150: 737-746.
37. Hameed, B.H., 2009a. Evaluation of papaya seeds as a novel non-conventional low-cost adsorbent for removal of methylene blue. J. Hazard. Mater., 162: 939-944.
38. Gholamreza, M. and K. Rasoul, 2010. The removal of cationic dyes from aqueous solutions by adsorptionontopistachiohullwaste.Chem.Eng. Res. Design. doi: 10.1016/j.cherd.2010.11.024.
39. Shukla, A., Y.H. Zhang, P. Dubey, J.L. Margrave and S.S. Shukla, 2002. The role of sawdust in the removal of unwanted materials from water. J. Hazard. Mater., B95 L: 137-152.
40. Han, R., W. Zou, W. Yu, S. Cheng, Y. Wang and J. Shi, 2007. Biosorption of methylene blue from aqueous solution by fallen phoenix tree's leaves. J. Hazard. Mater., 141: 156-162.
41. Allen, S.J., Q. Gan, R. Matthews and P.A. Johnson, 2003. Comparison of optimised isotherm models for basic dye adsorption by kudzu. Bioresour. Technol., 88 : 143-152.
42. Freundlich, H.M.F., 1906. Über dye adsorption in lösungen. Z. Phys. Chem. 57A : 385-470. 43. Pearce, C.I. J.R. Lloyd and J.T. Guthrie, 2003. Biodegradation of Azo dyes. Dyes Pigm. 58 : 179-196.
44. Temkin, M.J. and V. Pyzhev, 1940. Recent modifications to Langmuir isotherms. Acta Physiochim. USSR 12: 217-222.
45. Basar, C.A., 2006. Removal of direct blue-106 dye from aqueous solution using new activated carbons developed from pomegranate peel: Adsorption equilibrium and kinetics. J. Hazard. Mater., B135 : 232-241.
46. Singh, K.P., D. Mohan, S. Sinha, G. S. Tondon and D. Gosh, 2003. Color Removal from Wastewater Using Low- Cost Activated Carbon Derived from Agricultural Waste Material. Ind. Eng. Chem. Res., 42: 1965-1976.
47. Annadurai, G., 2002. Adsorption of Basic Dye on Strongly Chelating Polymer: Batch Kinetics Studies. Iranian Polynter J., 2: 237-244.
48. Vadivelan, V. and K. Vasanthkumar, 2005. Kinetics of adsorption of crystal violet from aqueous solutions using different natural materials. J. Colloid Inter. Sci., 91: 286.
49. Hamdaoui, O., 2006. Removal of rhodamine B from aqueous solutions by tea waste. J. Hazard. Mater., 135: 264-273.
50. Almeida, C.A.P., N.A. Debacher, A.J. Downs, L.C. Cottet and A.D. Mello, 2009. Removal of methylene blue from colored effluents by adsorption on montmorillonite clay. J. Colloid Interface Sci., 332: 46-53.
51. Gupta, V.K., A. Mittal, A. Malviya and J. Mittal, 2009. Adsorption of Carmoisine o from Wastewater Using Waste Materials-Bottom Ash and Deoiled Soya. J. Colloid and Interface Sci., 335: 24-33.
52. Mall, I.D., V.C. Srivastava, N.K. Agarwa and I.M. Mish, 2005. Adsorptive Removal of Malachite Green Dye from Aqueous Solution by Bagasse Fly Ash and Activated Carbon- Kinetic Study and Equilibrium Isotherm Analyses. Colloids Surf. A. 264: 17-28.
53. Abd El-Latif, M.M., A.M. Ibrahim and M.F. El-Kady, 2010. Adsorption Equilibrium, kinetics and thermodynamics of methylene blue from aqueous solutions using biopolymer oak sawdust composite, J. American Sci., 6: 6.